Inherent Selectivity of Pd C-H Activation from Different Metal Oxidation States

Peter Amadeo,[‡] Bangaru Bhaskararao,[‡] Yun-Fang Yang,[§] Marisa C. Kozlowski[‡,*]

[‡]Department of Chemistry, University of Pennsylvania, Philadelphia, Pennsylvania 19104, United States.

[§]College of Chemical Engineering, Zhejiang University of Technology, Hangzhou, Zhejiang 310014, China.

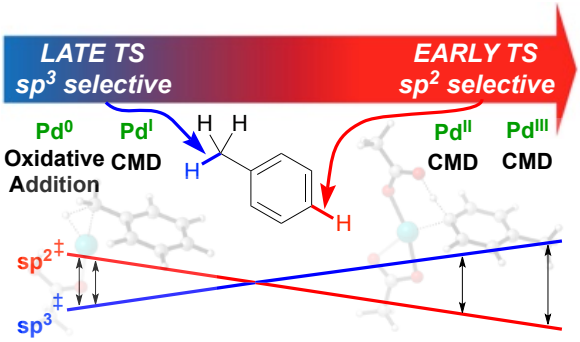

ABSTRACT: In investigating potential control factors that would permit a palladium-catalyzed benzylic vs arene C–H activation as previously reported by our group, it was discovered that the oxidation state of the homogenous palladium species influences the selectivity of C–H activation. DFT calculations show that Pd^0 and Pd^I preferentially activate the sp^3 C–H bond in toluene, whereas Pd^{II} and Pd^{III} preferentially activate the sp^2 C–H bond. This selectivity appears to originate from the steric environment created by the ligand framework on the palladium. As the palladium oxidation state increases, the number of ligand sites increases, which decreases the energetic favorability for activation of the weaker, yet more hindered sp^3 C–H bond.

INTRODUCTION

As C–H activation grows as a field, the nuance of selective activation is of increasing interest. A large number of C–H bonds have successfully undergone Pd–mediated activation through a variety of processes. The vast majority of these processes involve Pd(II) concerted metalation deprotonation (CMD) which inherently favors sp^2 hybridized carbons vs. sp^3 hybridized carbons.[1,2,3] This selectivity can be reversed by means of a directing group[4,5,6] in CMD processes (Scheme 1a-b) or by utilizing radical processes to first abstract a hydrogen and then intercepting the carbon centered radical at a metal center (Scheme 1c).[7,8]

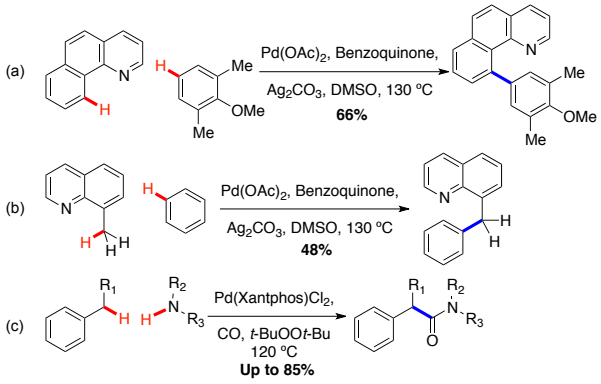

Scheme 1. Examples of C–H activation by directing group of an arene C–H bond (a) and a benzylic C–H bond (b) as well as by free radical hydrogen atom abstraction (c).

Recent research has shown that oxidation states of Pd asides from Pd^0 and Pd^{II} are accessible including Pd^I,[9,10] Pd^{III},[11,12,13] and Pd^{IV} (Scheme 2).[14] This article investigates the inherent activation selectivity for sp^2 vs. sp^3 hybridized carbons computationally using four oxidation states of Pd and sets the stage for further study of

differentially selective processes with these systems.

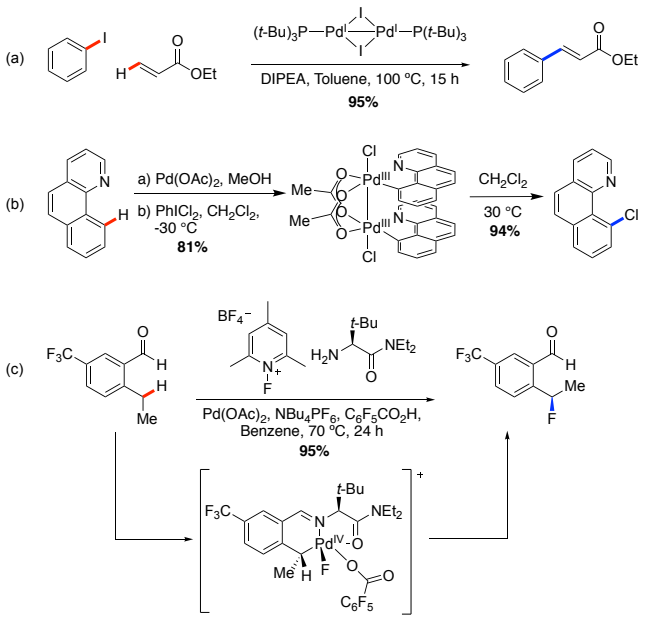

Scheme 2. Examples of C–H activation with palladium in oxidation states I (a), III (b), and IV (c).

We were motivated to study these processes based on findings from our laboratory that $Pd(OAc)_2$ would selectively activate the benzylic C-H of alkyl arenes (Scheme 3).[15,16] Since this selectivity is diametrically opposite of that reported for CMD with Pd^{II}, we became interested in determining if any homogeneous Pd catalysts would give rise to the observed selectivity. Thus, this study focuses on two C–H bonds in toluene: the benzylic sp^3 center and the least hindered arene sp^2 center which is *para* to the methyl group.

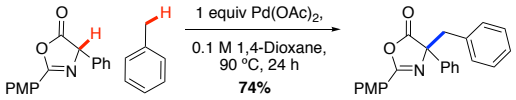

Scheme 3. Our previously reported palladium-catalyzed benzylic C–H activation.

RESULTS AND DISCUSSION

Concerted metalation deprotonation, a variant of σ-bond metathesis, is a well-known mode for Pd^{II} C–H activation where a basic ligand abstracts a proton while the Pd–C bond forms. This process is redox neutral and requires an anionic ligand. As such, the oxidation states Pd^{I}, Pd^{II}, and Pd^{III} were considered with this modality.[17] Another, C–H activation pathway is oxidative addition, which is rare in Pd chemistry.[18,19,20,21] In this process, the oxidation state of the palladium increases by two as the palladium breaks the C–H bond to form a Pd–C and a Pd–H bond. Oxidative addition was only considered here for Pd^0.

It is important to note that the activation energies cannot be compared between the oxidation states without specifying reaction conditions. The relative energies of the different oxidation states of palladium are dependent on the oxidant or reductant present, so the absolute barriers from a precursor common to all eight pathways will not be discussed.

All DFT calculations were carried out using Gaussian 16C.01.[22] The B3LYP[23,24] and then the M06[25] functional were used to explore conformational space and perform geometry optimizations, transition state optimizations, and frequency calculations. The 6-31G* basis set was used for atoms C, H, N, and O while the LANL2DZ ECP was used for Pd.[26,27] Single point calculations were carried out on optimized structures with the unrestricted M06 functional and the SMD solvation model[28] with toluene as the solvent. The 6-311+G** basis set was used for atoms C, H, N, and O while the LANL2DZ ECP was used for Pd. Conformational space was explored thoroughly with each structure by first determining the correct number of ligands and then performing successive dihedral scans to find the lowest energy. All geometry optimizations were confirmed by the presence of no negative frequencies, and all transition states were confirmed by the presence of one and only one negative frequency. Intrinsic reaction coordinate calculations were also undertaken to confirm each transition state.

The results of the transition state calculations are shown in Figure 1. For each transition state, a number of neutral AcOH ligands were coordinated to the palladium center to determine the most energetically favorable ligand sphere. $Pd^0$and Pd^I are stabilized by one AcOH ligand, but Pd^{II} and Pd^{III} are most stable with the number of anionic acetate ligands corresponding to the respective oxidation states.

There is a notable trend moving progressively from an endergonic process to a more and more exergonic process as the oxidation state increases. In every case, formation of the benzylic adduct (sp^3 activation) is more thermodynamically favorable due to π-coordination. The transition state barriers of the C-H activation process also increase as the oxidation states increase.

With respect to selectivity, Pd^0 exhibited a barrier 2.9 kcal/mol lower for sp^3 activation than sp^2 activation. These results indicate a direct oxidative addition mechanism would afford selectivity complementary to Pd^{II} CMD. Overall, Pd^0 favors oxidative addition to the weakest bond (benzylic CH BDE = 85 kcal/mol, arene CH BDE = 103 kcal/mol).[29] For Pd^I, CMD also favors the sp^3 activation by 3.4 kcal/mol. However, for Pd^{II} sp^2 activation becomes more preferable by 3.4 kcal/mol in accord with prior calculations.[30] For Pd^{III}, the same trend is observed, but the gap increases to 5.7 kcal/mol.

An examination of the bond lengths (Table 1) indicates the largest degree of C–H bond cleavage in the Pd^0 transition states (1.92/1.71 Å) relative to the toluene C-H bonds (1.08/1.09 Å). As

Table 1. Transition State C–H Bond Lengths[a]

Oxidation state	TS sp^2 C–H (Å)	TS sp^3 C–H(Å)
Pd^0	1.92	1.71
Pd^I	1.41	1.41
Pd^{II}	1.30	1.32
Pd^{III}	1.26	1.27

[a]M06/6-31G*/LANL2DZ

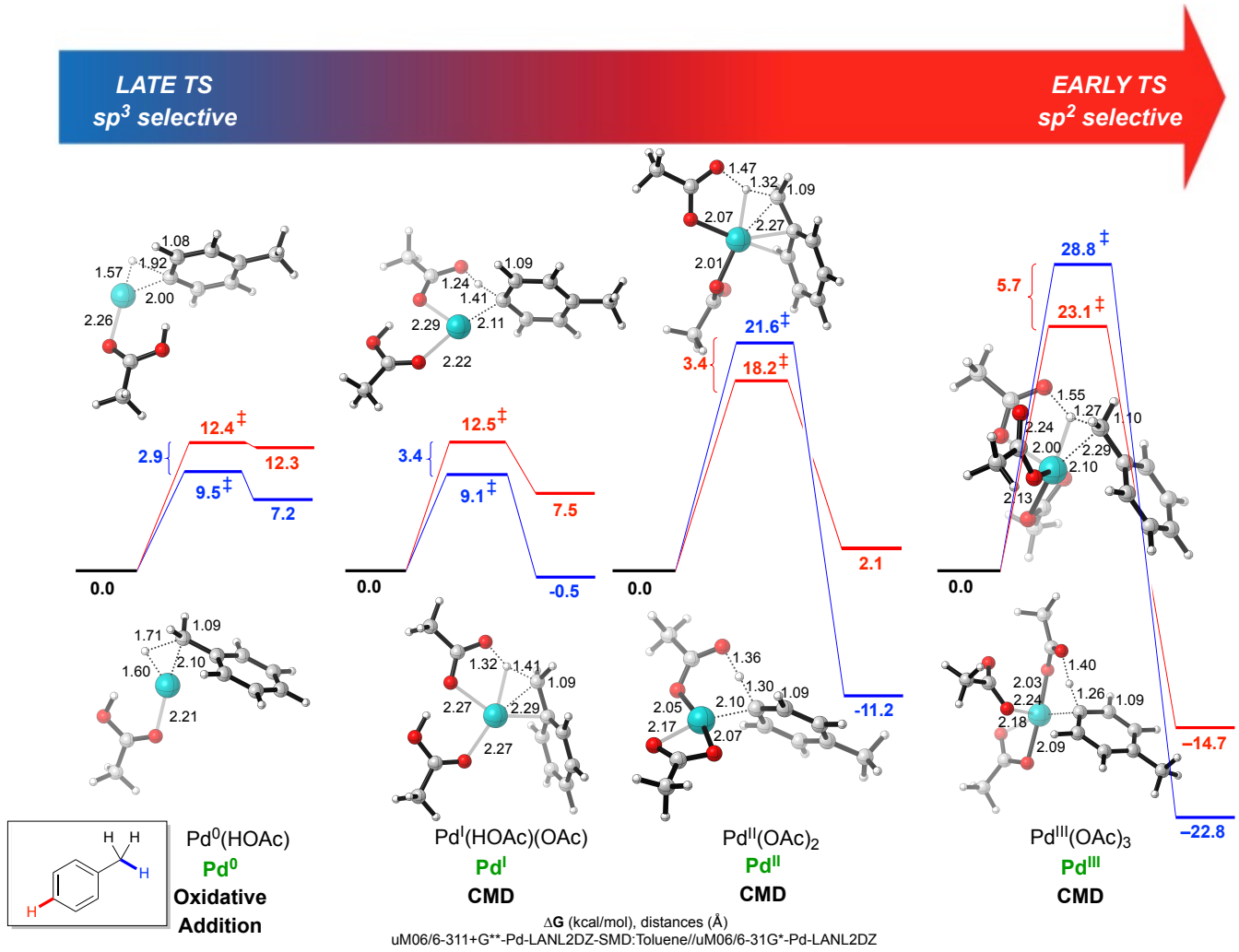

Figure 1. Transition states and relative barriers for toluene activation with different Pd species (sp^3 shown in blue, sp^2 shown in red).

Table 2. Distortion-Interaction Electronic Energies[a]

Oxidation state	TS sp^2					TS sp^3				
	E_d(Pd)	E_d($PhCH_3$)	E_d(tot)	E_i	E_{act}	E_d(Pd)	E_d($PhCH_3$)	E_d(tot)	E_i	E_{act}
Pd^0	1.0	88.5	89.5	–86.4	3.1	0.1	58.2	58.3	–58.4	–0.1[a]
Pd^I	3.4	34.7	38.1	–41.7	–3.6[a]	0.8	28.7	29.5	–35.3	–5.8[a]
Pd^{II}	27.5	28.5	56.0	–48.2	7.8	46.3	20.6	66.9	–51.4	15.5
Pd^{III}	36.9	25.7	62.6	–48.8	13.8	32.6	18.3	50.9	–29.9	21.0

[a] M06/6-31G*/LANL2DZ, kcal/mol. [b]Negative values arise from lack of entropic and thermal corrections and comparison to separated starting materials rather than coordination adducts (c.f. Figure 1).

such, these transitions states are the latest. There is a trend where the transition state C–H bond lengths progressively shorten moving from Pd^0 to Pd^{III}, with the latter having the earliest transition states. These observations are in accord with the overall thermodynamics;

namely, the Hammond postulate would indicate that more endergonic reactions would have later transitions states, as is the case for Pd^0, while more exergonic reactions would have earlier transition states, as is the case for Pd^{III}. The Pd^I and Pd^{II} transitions states are intermediate to these extremes.

There are numerous studies supporting that "C-H activating systems generally exhibit thermodynamic as well as kinetic preferences for aromatic over benzylic activation,"[31,32] However, the data in Figure 1 show a potentially more complex scenario within the Pd manifold. To gain better insight into the reasons behind the computed selectivity values, a distortion interaction energy analysis[33] was performed by comparing the transition states to the ground states of the separated components (Table 2, Figure 2). The overall electronic energies confirm that sp^3 activation is more favorable for Pd^0 oxidation addition and Pd^I CMD, while sp^2 activation is favored for the Pd^{II} and Pd^{III} CMD. In general, the interaction energies are strongest for sp^2 activation indicating that the potential stabilization from π-coordination of the benzylic portion is not dominant in the transition states. Rather, the interaction of Pd with sp^2 carbons is stronger than sp^3 carbons, which is at least partly a reflection of the stronger Pd-C(sp^2) bond strength.[34] Interaction energies are strongest for Pd^0 which likely reflects greater back-bonding from the low valent metal center.

Figure 2. Distortion-interaction diagram for toluene activation.

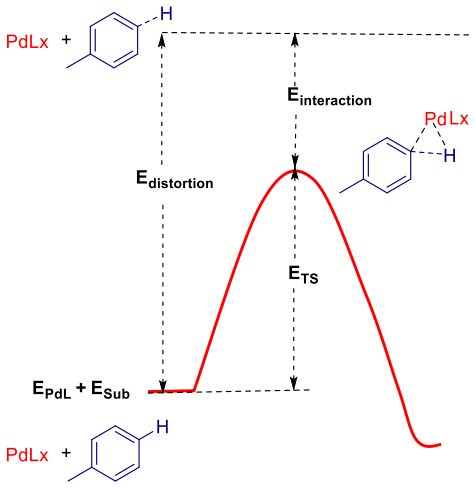

For Pd^0 and Pd^I, there is almost no distortion of the Pd portions in any of the transition states indicating the largely unhindered nature of these low coordinate species. However, the distortion energies of the overall transition states are high (29.5-89.5 kcal/mol) due to the toluene portion. For late transition states, significant distortion of the toluene portion from the ground state aligns with this finding. The distortion energy of the sp^2 center of toluene is far higher (34.7-88.5 kcal/mol) than that of the sp^3 center (28.7-58.2 kcal/mol), which likely reflects both the stronger sp^2 C—H bond and a reduction of aromaticity in the reaction of the sp^2 carbon that would arise from a p-orbital of the aromatic π-system participating in the formation of the new Pd–C bond. This effect can be seen in the distortion of the sp^2 C—H bond out the aromatic plane in the transition state. Such an interaction does not occur with the sp^3 carbon. It is striking the these higher sp^2distortion energies are so large that they both offset the higher sp^2 interaction energy and destabilize the transition states relative to the sp^3 activation. All told, the selective activation of the sp^3 centers by Pd^0 and Pd^I is both kinetic and thermodynamically favored due to lesser distortion of the sp^3 center upon coordination and reaction.

For Pd^{II} and Pd^{III}, there is a large amount of distortion in the Pd portions (27.5-46.3) indicating that significant rearrangement of the coordination sphere is needed from the reactants to the transition state. The overall distortion energies from Pd^{II} and Pd^{III} are of similar magnitudes to those from Pd^0 and Pd^I. As a consequence, the toluene distortion energies are smaller for Pd^{II} and Pd^{III} (18.3-28.5 kcal/mol). As these transition states are earlier, there is less perturbation of the toluene from its ground state and accordingly lower distortion energies. Although there is less distortion for the toluene portion in the sp^3 activation, the interaction energies and Pd distortion energies combine to disfavor sp^3 activation relative to sp^2 activation. Because the transition states are earlier there is no longer as strong a penalty from loss of aromaticity in the toluene portion upon sp^2 activation. Notably, the thermodynamic products appear to be the sp^3 activation adducts which are stabilized by benzylic π-coordination; however, the early nature of the transition states precludes this factor from being decisive with respect to the transition state energies. All told, these Pd^{II} and Pd^{III} species are more hindered than their Pd^0 and Pd^I analogs resulting in more favorable reaction with the less hindered trigonal carbon that also benefits from forming a stronger bond to the metal.

CONCLUSION

Ligand design Pd^0 product structures better for ligand design; ligand can be more distal since Pd-C is largely formed and shorter in TS, however need to have a larger ligand due to the openness of the Pd center. For Pd^{II} and Pd^{III}, precordination complexes more relevant, ligands need to intimately interact with incoming substrate, can adjust the electrophilicity with cationic complexes

The selectivity trends discovered herein set the stage for designing future catalysts. For example, ligands could be incorporated to shift the transition states from early to late or vice versa to favor selective activation of different centers. With Pd^{II} and Pd^{III}, selection of ligands that destabilize the product could potentially shift selectivity. This work also how C-H activation from Pd^0 and Pd^I could lead to novel reactivity profiles. Overall, ligand frameworks and reaction conditions (e.g. electrochemical) to access these different redox couples with Pd and related elements will allow the fundamental drivers of selectivity to be modified. Such studies would allow even greater control over selectivity in C-H activation, considered one of the Holy Grails in synthetic methods development.[35,36]

ASSOCIATED CONTENT

Computational methods and thermochemical data. This material is available free of charge via the Internet at http://pubs.acs.org.

AUTHOR INFORMATION

Corresponding Author

* E-mail: marisa@sas.upenn.edu

Notes

The authors declare no competing financial interest.

ACKNOWLEDGMENT

We are grateful to the NIH (R35 GM131902) and NSF (CHE1764298) for financial support of this research. We acknowledge XSEDE (TGCHEM120052) for computational resources. We thank Prof. Xin Hong (Zhejiang Univ.) for helpful discussions.

Keywords

C-H activation • palladium catalysis • concerted metalation deprotonation • DFT

REFERENCES

1 Fagnou, K.; Lapointe, D. Overview of the Mechanistic Work on the Concerted Metallation-Deprotonation Pathway *Chem. Lett.* **2010**, *39*, 1118–1126.

2 Yeung, C. S.; Dong, V. M. Catalytic Dehydrogenative Cross-Coupling: Forming Carbon–Carbon Bonds by Oxidizing Two Carbon–Hydrogen Bonds *Chem. Rev.* **2011**, *111*, 1215–1292.

3 He, J.; Wasa, M.; Chan, K. S. L.; Shao, Q.; Yu, J. Palladium-Catalyzed Transformations of Alkyl C–H Bonds *Chem. Rev.* **2017**, *117*, 8754–8786.

4 Hull, K. L.; Sanford, M. S. Catalytic and Highly Regioselective Cross-Coupling of Aromatic C–H Substrates *J. Am. Chem. Soc.* **2007**, *129*, 11904–11905.

5 Lyons, T. W.; Sanford, M. S. Palladium-Catalyzed Ligand-Directed C–H Functionalization Reactions *Chem. Rev.* **2010**, *110*, 1147–1169.

6 Neufeldt, S. R.; Sanford, M. S. Controlling Site Selectivity in Palladium-Catalyzed C–H Bond Functionalization *Acc. Chem. Res.* **2012**, *45*, 936–946.

7 Xie, P.; Xia, C.; Huang, H. Palladium-Catalyzed Oxidative Aminocarbonylation: A New Entry to Amides via C–H Activation *Org. Lett.* **2013**, *15*, 3370–3373.

8 Xie, P.; Xie, Y.; Qian, B.; Zhou, H.; Xia, C.; Huang, H. Palladium-Catalyzed Oxidative Carbonylation of Benzylic C–H Bonds via Nondirected C(sp^3)–H Activation *J. Am. Chem. Soc.* **2012**, *134*, 9902–9905.

9 Proutiere, F.; Aufiero, M.; Schoenebeck, F. Reactivity and Stability of Dinuclear Pd(I) Complexes: Studies on the Active Catalytic Species, Insights into Precatalyst Activation and Deactivation, and Application in Highly Selective Cross-Coupling Reactions *J. Am. Chem. Soc.* **2012**, *134*, 606–612.

10 Stirner, C. K.; Schoenebeck, F.; Sperger, T. Bench-Stable and Recoverable Palladium(I) Dimer as an Efficient Catalyst for Heck Cross-Coupling *Synthesis* **2017**, *49*, 115–120.

11 Powers, D. C.; Ritter, T. A Transition State Analogue for the Oxidation of Binuclear Palladium(II) to Binuclear Palladium(III) Complexes *Organometallics* **2013**, *32*, 2042–2045.

12 Powers, D. C.; Benitez, D.; Tkatchouk, E.; III, W. A. G.; Ritter, T. Bimetallic Reductive Elimination from Dinuclear Pd(III) Complexes *J. Am. Chem. Soc.* **2010**, *132*, 14092–14103.

13 Powers, D. C.; Ritter, T. Bimetallic Pd(III) complexes in palladium-catalysed carbon–heteroatom bond formation *Nat. Chem.* **2009**, *1*, 302-309.

14 Park, H.; Verma, P.; Hong, K.; Yu, J. Controlling Pd(IV) reductive elimination pathways enables Pd(II)-catalysed enantioselective C(sp^3)–H fluorination *Nat. Chem.* **2018**, *10*, 755–762.

15 Curto, J. M.; Kozlowski, M. C. Chemoselective Activation of sp^3 vs sp^2 C–H Bonds with Pd(II) *J. Am. Chem. Soc.* **2015**, *137*, 18–21.

16 Hong, G.; Nahide, P. D.; Neelam, U. K.; Amadeo, P.; Vijeta, A.; Curto, J. M.; Hendrick, C. E.; Vangelder, K. F.; Kozlowski, M. C. Palladium-Catalyzed Chemoselective Activation of sp^3 vs sp^2 C–H Bonds: Oxidative Coupling To Form Quaternary Centers *ACS Catal.* **2019**, *9*, 3716–3724.

17 Only acetate assisted intramolecular variants of the CMD transistion states were considered as they have been found to be lowest in energy. See reference 1.

18 Gilbert, T. M.; Hristov, I.; Ziegler, T. Comparison between Oxidative Addition and σ-Bond Metathesis as Possible Mechanisms for the Catalytica Methane Activation Process by Platinum(II) Complexes: A Density Functional Theory Study *Organometallics* **2001**, *20*, 4633–4639.

19 Nag, N. K. A Study on the Formation of Palladium Hydride in a Carbon-Supported Palladium Catalyst *J. Phys. Chem.* **2001**, *105*, 5945–5949.

20 Chin, Y. C.; Buda, C.; Neurock, M.; Iglesia, E. Consequences of Metal–Oxide Interconversion for C–H Bond Activation during CH_4 Reactions on Pd Catalysts *J. Am. Chem. Soc.* **2013**, *135*, 15425–15442.

21 Diefenbach, A.; Bickelhaupt, F. M. Activation of H–H, C–H, C–C, and C–Cl Bonds by Pd(0). Insight from the Activation Strain Model *J. Phys. Chem. A* **2004**, *108*, 8460–8466.

22 Frisch, M. J.; Trucks, G. W.; Schlegel, H. B.; Scuseria, G. E.; Robb, M. A.; Cheeseman, J. R.; Scalmani, G.; Barone, V.; Mennucci, B.; Petersson, G. A.; Nakatsuji, H.; Caricato, M.; Li, X.; Hratchian, H. P.; Izmaylov, A. F.; Bloino, J.; Zheng, G.; Sonnenberg, J. L.; Hada, M.; Ehara, M.; Toyota, K.; Fukuda, R.; Hasegawa, J.; Ishida, M.; Nakajima, T.; Honda, Y.; Kitao, O.; Nakai, H.; Vreven, T.; Montgomery, J. A., Jr.; Peralta, J. E.; Ogliaro, F.; Bearpark, M.; Heyd, J. J.; Brothers, E.; Kudin, K. N.; Staroverov, V. N.; Kobayashi, R.; Normand, J.; Raghavachari, K.; Rendell, A.; Burant, J. C.; Iyengar, S. S.; Tomasi, J.; Cossi, M.; Rega, N.; Millam, N. J.; Klene, M.; Knox, J. E.; Cross, J. B.; Bakken, V.;Adamo, C.; Jaramillo, J.; Gomperts, R.; Stratmann, R. E.; Yazyev, O.; Austin, A. J.; Cammi, R.; Pomelli, C.; Ochterski, J. W.; Martin, R. L.; Morokuma, K.; Zakrzewski, V. G.; Voth, G. A.; Salvador, P.;Dannenberg, J. J.; Dapprich, S.; Daniels, A. D.; Farkas, Ö.;Foresman, J. B.; Ortiz, J. V.; Cioslowski, J.; Fox, D. J. Gaussian 16, Revision C.01; Gaussian, Inc., Wallingford CT, 2019.

23 Becke, A. D. Density-functional thermochemistry. III. The role of exact exchange *J. Chem. Phys.* **1993**, *98*, 5648–5652.

24 Kohn, W.; Becke, A. D.; Parr, R. G. Density Functional Theory of Electronic Structure *J. Phys. Chem.* **1996**, *100*, 12974–12980.

25 Zhao, Y.; Truhlar, D. G. The M06 suite of density functionals for main group thermochemistry, thermochemical kinetics, noncovalent interactions, excited states, and transition elements: two new functionals and systematic testing of four M06-class functionals and 12 other functionals *Theor. Chem. Acc.* **2008**, *120*, 215–241.

26 Hay, P. J.; Wadt, W. R. *Ab initio* effective core potentials for molecular calculations. Potentials for K to Au including the outermost core orbitals *J. Chem. Phys.* **1985**, *82*, 299–310.

27 Wadt, W. R.; Hay, P. J. *Ab initio* effective core potentials for molecular calculations. Potentials for the transition metal atoms Sc to Hg *J. Chem. Phys.* **1985**, *82*, 270–283.

28 Marenich, A. V; Cramer, C. J.; Truhlar, D. G. Universal Solvation Model Based on Solute Electron Density and on a Continuum Model of the Solvent Defined by the Bulk Dielectric Constant and Atomic Surface Tensions *J. Phys. Chem.* B **2009**, *113*, 6378–6396.

29 Benson, S. W. Bond Energies *J. Chem. Educ.* **1965**, *42*, 502–518.

30 Zhou, Y.; Wang, M.; Fang, S.; Chen, Y.; Liu, J. DFT studies on the mechanism of palladium catalyzed arylthiolation of unactive arene to diaryl sulfide *RSC Adv.* **2016**, *6*, 18300–18307.

31 Heyduk, A. F.; Driver, T. G.; Labinger, J. A.; Bercaw, J. E. Kinetic and Thermodynamic Preferences in Aryl vs Benzylic C–H Bond Activation with Cationic Pt(II) Complexes *J. Am. Chem. Soc.* **2004**, *126*, 15034–15035.

32 (a) Janowicz, A. H.; Bergman, R. G. Activation of C-H Bonds in Saturated Hydrocarbons on Photolysis of (775-C5Me5)(PMe3)IrH2. Relative Rates of Reaction of the Intermediate with Different Types of C-H Bonds and Functionalization of the Metal-Bound Alkyl Groups *J. Am. Chem. Soc.* **1983**, *105*, 3929-3939. (b) Jones, W. D.; Hessell, E. T. Photolysis of Tp/Rh(CN-neopentyl)(772-PhN=C=N-neopentyl) in Alkanes and Arenes: Kinetic and Thermodynamic Selectivity of [TpzRh(CN-neopentyl)] for Various Types of C-H Bonds *J. Am. Chem. Soc.* **1993**, *115*, 554-562. (c) Driver, T. G.; Day, M. W.; Labinger, J. A.; Bercaw, J. E. "Mechanism of C–H Bond Activation of Alkyl-Substituted Benzenes by Cationic Platinum(II) Complexes" *Organometallics* **2005**, *24*, 3644–3654. (d) Zhao, S. B.; Song, D.; Jia, W. L.; Wang, S. "Regioselective C–H Activation of Toluene with a 1,2-Bis(N-7-azaindolyl)benzene Platinum(II) Complex" *Organometallics* **2005**, *24*, 3290–3296. (e) Johansson, L.; Ryan, O. B.; Rømming, C.; Tilset, M. "Unexpected Selectivities in C–H Activations of Toluene and p-Xylene at Cationic Platinum(II) Diimine Complexes. New Mechanistic Insight into Product-Determining Factors" *J. Am. Chem. Soc.* **2001**, *123*, 6579–6590.

33 (a) Bickelhaupt, F. M. Understanding reactivity with Kohn–Sham molecular orbital theory: E2–S_N2 mechanistic spectrum and other concepts *J. Comput. Chem.* **1999**, *20*, 114-128. (b) Ess, D. H.; Houk, K. N. Distortion/Interaction Energy Control of 1,3-Dipolar Cycloaddition Reactivity *J. Am. Chem. Soc.* **2007**, *129*, 10646. (c) Bickelhaupt, F. M.; Houk. K. N. Analyzing Reaction Rates with the Distortion/Interaction-Activation Strain Model *Angew. Chem., Int. Ed.* **2017**, *56*, 10070.

34 Siegbahn, P. E. M. Trends of Metal-Carbon Bond Strengths in Transition Metal Complexes *J. Phys. Chem.* **1995**, *99*, 12723-12729.

35 Kozlowski, M. C. Oxidative Coupling in Complexity Building Transforms *Acc. Chem. Res.* **2017**, *50*, 638–643.

36 Yang, Y.; Hong, X.; Yu, J.; Houk, K. N. Experimental–Computational Synergy for Selective Pd(II)-Catalyzed C–H Activation of Aryl and Alkyl Groups *Acc. Chem. Res.* **2017**, *50*, 2853–2860.